mathematics

MDPI

Article

An Adaptive Controller Design for Nonlinear Active Air Suspension Systems with Uncertainties

Jinhua Zhang , Yi Yang and Cheng Hu *

School of Mechanical and Electrical Engineering, Guangzhou University, Guangzhou 510006, China
* Correspondence: c_hu@gzhu.edu.cn

Abstract: Active air spring suspensions can improve the vehicle ride comfort and meanwhile realize the vehicle height regulation, and therefore, they have been widely used and studied. However, to achieve better ride comfort and a satisfactory vehicle body height adjustment, the active air suspension controller becomes an indispensable and significant part of the system. Since the nonlinear suspension system possesses uncertainties, it is difficult to take into account both ride comfort and height regulation. This study innovatively proposes an adaptive control algorithm to specifically address the problem of vehicle height regulation and ride comfort for nonlinear active air suspension systems with uncertainties. The accurate tracking to reference vehicle body height curves is realized, and the ride comfort is also improved. Through simulations with two scenarios, it is illustrated that the active air suspension controller owns better control effectiveness than the PID controller. Compared with the PID controller, the designed controller can track the reference vehicle body height curves faster and more accurately. The result also verifies the priority of the designed controller.

Keywords: active air suspension; nonlinear systems; uncertainties; adaptive control; Lyapunov stability

MSC: 93-10

Citation: Zhang, J.; Yang, Y.; Hu, C. An Adaptive Controller Design for Nonlinear Active Air Suspension Systems with Uncertainties. *Mathematics* **2023**, *11*, 2626. https://doi.org/10.3390/math11122626

Academic Editors: Camelia Petrescu and Valeriu David

Received: 22 April 2023
Revised: 6 June 2023
Accepted: 7 June 2023
Published: 8 June 2023

1. Introduction

Automotive active suspension has been developed over the last few decades, and can be controlled via a computer. An excellent automotive active suspension possesses lots of advantages. Instead of driven suspension, the height of the car body above the ground is kept at a reasonable value by adjusting its own parameters [1]. In this way, the handling stability and the ride of the car can be highly improved through the appliance of automotive active suspensions. However, the high cost and the high hardware requirements limit the popularization and application of the automotive active suspension in automobiles.

Up to now, active suspension is gradually being widely used, and many papers have proposed control methods of active suspension, such as H-infinity control [2–5]. The literature [6] proposes a synergetic law of discontinuous control of the active suspension system of the car in order to reduce the influence of hysteresis and the dead zone. In the literature [7], the paper has designed event-trigger control for the fuzzy T-S systems with parameter uncertainties and disturbances. Simulations are given for the vehicle suspension systems. Control methods such as adaptive harmonic control [8], double time-delay feedback control [9] and nonlinear robust control [10] are adopted in active suspension research. The literature [11] applies the voice coil motor (VCM) to the active suspension in order to improve robustness of active suspension. Furthermore, the active suspension is not only applied in automotive, but is also adopted in other fields. The literature [12] outlines the potential for active suspensions in railway applications, and the literature [13] investigates the lateral stability of this mobile robot when it reconfigures itself to adjust its roll angle with the active suspension.

With the development of automobile suspension technology, people's requirements for vehicle riding comfort are also increasing. The appearance of automotive air suspension

meets people's needs [14,15]. The control link of the active suspension is equipped with a device that is capable of producing a jerk, which can inhibit the impact force of the road surface on the body and adjust the car body height [16]. The air suspension keeps the constant driving height of the vehicle on different road surfaces by adjusting the charging and discharging of the air suspension bag. The air suspension can also automatically adjust the height of the body according to the speed and set different vehicle damping. The research model of this paper is automotive air suspension. At the same time, many studies have performed research on air suspension. The literature [17] presents a new nonlinear adaptive sliding-mode control method for electronically controlled air suspension. The literature [18] focuses on the evaluation of the dynamic load reduction at all axles of a semi-trailer with an air suspension system. The literature [19] describes the structure and design principle of the air suspension system, and makes an analysis and a discussion on the key use effect, i.e., the damping effect. Different control methods are proposed, such as the semi-active control strategy of the vehicle [20] and interconnected state control [21].

In this paper,the backstepping method is used to design the controller. Its main idea is to recursively construct the Lyapunov function of the closed-loop system to obtain the feedback controller, and to select the control law to make the derivative of the Lyapunov function along the trajectory of the closed-loop system have a certain type of performance to ensure the boundedness and convergence of the trajectory of the closed-loop system to the equilibrium point. The method of backstepping is used in much of the literature. The literature [22] presents an adaptive backstepping sliding mode tracking control method for an underactuated unmanned surface vehicle. Adaptive backstepping is also adopted in nonlinear systems [23] and is designed for trajectory tracking and payload delivery in a medical emergency. In the literature [24], closed loop system characteristics with an incremental backstepping controller are investigated through theoretical analysis when both measurement biases and model uncertainties exist.

Adaptive control is also adopted to design the controller of the nonlinear air spring suspension. Adaptation is the ability of a system to change its behavior in order to adapt to a new environment. Therefore, adaptive control can be viewed as a feedback control system that can intelligently adjust its own characteristics in response to changes in the environment so that the system can work optimally according to some set criteria. The literature [25] presents a novel adaptive feedforward controller design for reset control systems. Furthermore, adaptive control has been applied in different fields and is used to study different objects [26,27].

From the above literature analysis, many references have proposed great control algorithms and have obtained excellent results. Although some reports have studied the air suspension system and have designed adaptive control algorithms; however, the uncertainties of nonlinear air suspension systems, which has become a difficult problem, are neglected by many designed control methods. Thus, this paper innovatively proposes an adaptive control algorithm to specifically address the problem of vehicle height regulation and ride comfort for nonlinear active air suspension systems with uncertainties. Under this control method, both ride comfort and vehicle height regulation can be taken into account when the uncertainty of a nonlinear system is considered.

The remainder of the paper is structured as follows. Section 2 established the controller based on adaptive backstepping. In Section 3, simulation is given to the controller. Two different road inputs are used to verify the controller effectiveness. Finally, Section 4 presents the conclusion of this research.

2. Problem Formulation and Controller Design

A physical model of automobile air suspension can be built as in Figure 1. Here, z_s is the vertical displacement of the sprung mass, z_w is the vertical displacement of the unsprung mass, z_r is the pavement vertical input, m_s is the sprung mass, m_w is the unsprung mass, c_s is the damping coefficient of the suspension shock absorber, c_w is the tire vertical

damping, k_w is vertical stiffness of the wheel table, and Q is the air mass flow through the solenoid valve.

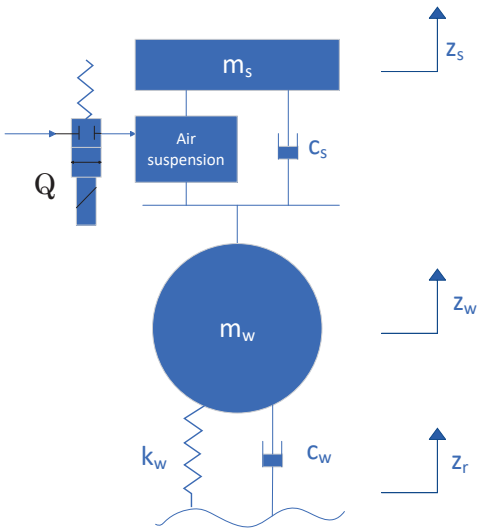

Figure 1. Physical model of air spring suspension.

According to the physical model shown in Figure 1, the dynamic model of sprung mass is established as

$$P_{\text{as}}A_{as} + c_s(\dot{z}_w - \dot{z}_s) + F_s = m_s\ddot{z}_s \tag{1}$$

where P_{as} is air spring chamber pressure, A_{as} is the effective cross-sectional area of the air spring, and F_s is the upper bound is known to be uncertain.

The dynamic model of the unsprung mass is

$$\begin{aligned} &k_w(z_r - z_w) + c_w(\dot{z}_r - \dot{z}_w) - P_{as}A_{as} \\ &- c_s(\dot{z}_w - \dot{z}_s) + F_w = m_s\ddot{z}_w \end{aligned} \tag{2}$$

where F_w is the upper bound is known to be uncertain. The dynamic model of the air pressure chamber of the air spring is

$$\dot{P}_{\text{as}}A_{as}(z_{a0} + z_s - z_w) = -KP_{\text{as}}A_{as}(\dot{z}_s - \dot{z}_w) + KRTQ + F_p \tag{3}$$

where z_{a0} is the air spring at the beginning of high degree, K is the variable index, R is the ideal gas constant, T is the gas temperature, F_p is the upper bound, a known uncertainty.

The above formula can be sorted out:

$$\begin{cases} \dot{P}_{\text{as}} &= \frac{KRT}{A_{as}(z_{a0}+z_s-z_w)}Q - \frac{KP_{as}}{z_{a0}+z_s-z_w}(\dot{z}_s - \dot{z}_w) \\ & \quad + \frac{F_p}{A_{as}(z_{a0}+z_s-z_w)} \\ \ddot{z}_s &= \frac{A_{as}}{m_s}P_{as} + \frac{c_s}{m_s}(\dot{z}_w - \dot{z}_s) + \frac{F_s}{m_s} \\ \ddot{z}_w &= \frac{k_w}{m_w}(z_r - z_w) + \frac{c_w}{m_w}(\dot{z}_r - \dot{z}_w) - \frac{A_{as}}{m_s}P_{as} \\ & \quad - \frac{c_s}{m_w}(\dot{z}_w - \dot{z}_s) - \frac{F_w}{m_w} \end{cases} \tag{4}$$

Let $x_1 = z_s$, $x_2 = \dot{z}_s$, $x_3 = z_w$, $x_4 = \dot{z}_w$, $x_5 = P_{as}$, $x_6 = \frac{A_{as}}{m_s}\dot{x}_5 + \frac{c_s}{m_s}(x_4 - x_2)$, $Q = u$, $\frac{F_s}{m_s} = F_1$, $\frac{F_s}{m_w} = F_3$, $\frac{F_p}{m_s(z_{a0}+z_s-z_w)} = F_2$.

$$\begin{cases} \dot{x}_1 = x_2 \\ \dot{x}_2 = x_6 + F_1 \\ \dot{x}_3 = x_4 \\ \dot{x}_4 = \frac{k_w}{m_w}(z_r - x_3) + \frac{c_w}{m_w}(\dot{z}_r - x_4) - \ddot{x}_{1r} + F_3 \\ \dot{x}_6 = \frac{\mathrm{k}RT}{m_s(z_{a0}+x_1-x_3)}u + \frac{c_s}{m_s}(\dot{x}_4 - \dot{x}_2) + F_2 \\ -\frac{k}{z_{a0}+x_1-x_3}(x_6 - \frac{c_s}{m_s}(x_4 - x_2))(x_2 - x_4) \end{cases} \tag{5}$$

The control objective is to design controller u, which can make $x_1 \to x_{1r}$ and stabilize the system. Let $z_1 = x_1 - x_{1r}$, $z_2 = x_2 - x_{2r}$; x_{2r} is a virtual control input. Design $x_{2r} = -\tilde{F}_1 - k_1 z_1 + \dot{x}_{1r}$, where $\hat{F}_1$ is the estimated value of F_1, and $\tilde{F}_1$ is the error between the true value and the estimated value, which can easily have $\tilde{F}_1 = F_1 - \hat{F}_1$

$$\begin{aligned} \dot{z}_1 &= \dot{x}_1 - \dot{x}_{1r} \\ &= z_2 + x_{2r} - \dot{x}_{1r} \\ &= z_2 - \tilde{F}_1 - k_1 z_1 \end{aligned} \tag{6}$$

Design the Lyapunov function $V_1 = \frac{1}{2}{z_1}^2 + \frac{1}{2}\gamma_1^{-1}\widetilde{F}_1^2$

$$\begin{aligned} \dot{V}_1 &= z_1\dot{z}_1 + \gamma_1^{-1}\tilde{F}_1\dot{\tilde{F}}_1 \\ &= z_1 z_2 - k_1 z_1^2 - \tilde{F}_1(z_1 + \gamma_1^{-1}\dot{\hat{F}}_1) \end{aligned} \tag{7}$$

The dynamic equation of z_2

$$\begin{aligned} \dot{z}_2 &= \dot{x}_2 - \dot{x}_{2r} \\ &= x_6 + F_1 - \dot{\hat{F}}_1 + k_1\dot{z}_1 - \ddot{x}_{1r} \end{aligned} \tag{8}$$

Let $z_3 = x_6 - x_{6r}$; x_{6r} is also the virtual control input.
Design

$$x_{6r} = -\mathrm{k}_2 z_2 - z_1 - k_1\dot{z}_1 + \ddot{x}_{1r} - \hat{F}_1 - \tilde{F}_2 + \phi_1 \tag{9}$$

where ϕ_1 is a tuning function, which is undetermined, and $\tilde{F}_2 = F_2 - \hat{F}_2$. Design the Lyapunov function $V_2 = \frac{1}{2}{z_2}^2 + \frac{1}{2}\gamma_2^{-1}\widetilde{F}_2^2 + V_1$

$$\begin{aligned} \dot{V}_2 =& z_2\dot{z}_2 + \gamma_2^{-1}\tilde{F}_2\dot{\tilde{F}}_2 + \dot{V}_1 \\ =& z_2 z_3 - k_2 z_2^2 - k_1 z_1^2 - \tilde{F}_2(z_2 + \gamma_2^{-1}\dot{\hat{F}}_2) + z_2\gamma_1(\phi_2\gamma_1^{-1} - \gamma_1^{-1}\dot{\hat{F}}_1) \\ &+ \tilde{F}_1(z_2 - z_1 - \gamma_1^{-1}\dot{\hat{F}}_1) \end{aligned} \tag{10}$$

Let

$$\phi_1 = \gamma_1(z_2 - z_1) \tag{11}$$

Combining $\phi_1 = \gamma_1(z_2 - z_1)$ and Equation (10), we can have

$$\dot{V}_2 = z_2 z_3 - k_2 z_2^2 - k_1 z_1^2 - \tilde{F}_2(z_2 - \gamma_2^{-1}\dot{\hat{F}}_2) + (\tilde{F}_1 + z_2\gamma_1)(z_2 - z_1 - \gamma_1^{-1}\dot{\hat{F}}_1) \tag{12}$$

The dynamic equation of z_3

$$\begin{aligned} \dot{z}_3 =& \dot{x}_6 - \dot{x}_{6r} \\ =& \frac{\mathrm{k}RT}{m_s(z_{a0} + x_1 - x_3)}u + \frac{c_s}{m_s}(\dot{x}_4 - \dot{x}_2) + F_2 \\ &- \frac{k}{z_{a0} + x_1 - x_3}(x_6 - \frac{c_s}{m_s}(x_4 - x_2))(x_2 - x_4) \\ &- \dot{x}_{6r} \end{aligned} \tag{13}$$

Design

$$\begin{aligned} u = &- \frac{m_s(z_{a0}+x_1-x_3)}{\mathrm{k}RT}\Big(\frac{c_s}{m_s}(\dot{x}_4-\dot{x}_2)+\hat{F}_2 \\ &- \frac{k}{z_{a0}+x_1-x_3}\Big(x_6-\frac{c_s}{m_s}(x_4-x_2)\Big)(x_2-x_4)+k_2\dot{z}_2 \\ &+ \dot{z}_1+k_1\ddot{z}_1-\dddot{x}_{1r}-\dot{\phi}_1+k_3z_3+z_2-\phi_2-\phi_3\Big), \end{aligned} \tag{14}$$

where ϕ_2 and ϕ_3 are also undetermined tuning functions. Plugging u into (13) yields

$$\dot{z}_3 = -\dot{\hat{F}}_2+\dot{\hat{F}}_1+\tilde{F}_2-k_3z_3-z_2+\phi_2+\phi_3 \tag{15}$$

Design $V_3 = \frac{1}{2}{z_3}^2+V_2$

$$\begin{aligned} \dot{V}_3 =& z_3\dot{z}_3+\dot{V}_2 \\ =& z_3\gamma_2(\phi_3\gamma_2^{-1}-\gamma_2^{-1}\dot{\hat{F}}_2)+\tilde{F}_2(z_3-z_2-\gamma_2^{-1}\dot{\hat{F}}_2) \\ &+ z_3\gamma_1(\phi_2\gamma_1^{-1}+\gamma_1^{-1}\dot{\hat{F}}_1)+(\tilde{F}_1+z_2\gamma_1)(z_2 \\ &- z_1-\gamma_1^{-1}\dot{\hat{F}}_1)-\sum_{i=1}^{3}k_iz_i^2 \end{aligned} \tag{16}$$

Let $\phi_2 = \gamma_1(z_1-z_2)$,$\phi_3 = \gamma_2(z_3-z_2)$

$$\begin{aligned} \dot{V}_3 =& (\tilde{F}_2+z_3\gamma_2)(z_3-z_2-\gamma_2^{-1}\dot{\hat{F}}_2) \\ &+ (\tilde{F}_1+z_2\gamma_1-z_3\gamma_1)(z_2-z_1-\gamma_1^{-1}\dot{\hat{F}}_1)-\sum_{i=1}^{3}k_iz_i^2 \end{aligned} \tag{17}$$

Design $\dot{\hat{F}}_1 = (z_2-z_1)\gamma_1$ and $\dot{\hat{F}}_2 = (z_3-z_2)\gamma_2$, which leads to $\dot{V}_3 \leq 0$. According to Barbalat's lemma, we can have z_i approaches 0 when t approaches infinity.

When $\ddot{z}_1 = \dot{z}_2 = \dot{z}_3 = 0$, the system zero dynamics is

$$\begin{cases} \dot{x}_3 = x_4 \\ \dot{x}_4 = \frac{k_w}{m_w}(z_r-x_3)+\frac{c_w}{m_w}(\dot{z}_r-x_4)-\ddot{x}_{1r}+F_3 \end{cases} \tag{18}$$

it can be inferred

$$\ddot{x}_3+\frac{c_w}{m_w}\dot{x}_3+\frac{k_w}{m_w}x_3+\ddot{x}_{1r}-\frac{c_w}{m_w}\dot{z}_r+\frac{k_w}{m_w}z_r-F_3 = 0 \tag{19}$$

The characteristic equation is

$$s^2+\frac{c_w}{m_w}s+\frac{k_w}{m_w} = 0 \tag{20}$$

As $c_w > 0, k_w > 0, m_w > 0$, $\frac{c_w}{m_w} > 0$, $\frac{k_w}{m_w} > 0$ can be inferred. The coefficients of the characteristic equation of the second-order zero-dynamic system are all positive, so the zero-dynamic system is stable. x_3, x_4 is bounded when the road inputs that the value of $z_r, \dot{z}_r$, the reference signal $\ddot{x}_{1r}$ and uncertainty F_3 are bounded.

3. Simulation Verification

In order to verify the effectiveness of the adaptive control method, simulation verification is carried out. There are two scenarios. The first case is the pavement vertical input $z_r = 0.01\sin 2\pi t$ and $x_{1r} = 0.01\sin 2\pi t$. The other case is $x_{1r} = 0$, and the pavement vertical input is random. The vehicle parameters in simulation are shown in Table 1 below. The controller parameters are shown in Table 2 below [28].

Table 1. Vehicle parameters.

Parament	Value	Parament	Value
m_s	1535 kg	m_w	400 kg
c_w	10,000 Ns/m	k_w	650,000 Ns/m
c_s	11,086 Ns/m	K	1.4
T	293.15 k	R	287.1

Table 2. Controller design parameters.

Parament	Value	Parament	Value
k_1	100	k_2	100
γ_1	100	γ_2	100

3.1. Sinusoidal Road Input

In the sinusoidal road input simulation process, the parameters are set as follows. The vehicle height was adjusted under a vertical input of $z_r = 0.01 \sin 2\pi t$, the initial height of air sprung $z_{a0} = 0.03$ m, the uncertain outer boundary perturbation input $F_1(t) = F_2(t) = 0.01$, x_1 is initialized as 0.2 m, and other states are initialized to 0. The sampling time is 0.001 s and the simulation results are shown in Figures 2–7.

Figure 2 shows the tracing effect of the car body height on the reference trajectory in the process of vehicle height adjustment. Under control of the controller, the tracing curve of the car body height almost coincides with reference trajectory. As $z_1 = x_1 - x_{1r}$, $z_1 = 0$ can be inferred. Figure 3 is the curve of z_1, which confirms $z_1 = 0$. Compared with the PID controller, the designed controller can not only track the reference curve more accurately, but also make the error more inclined to 0.

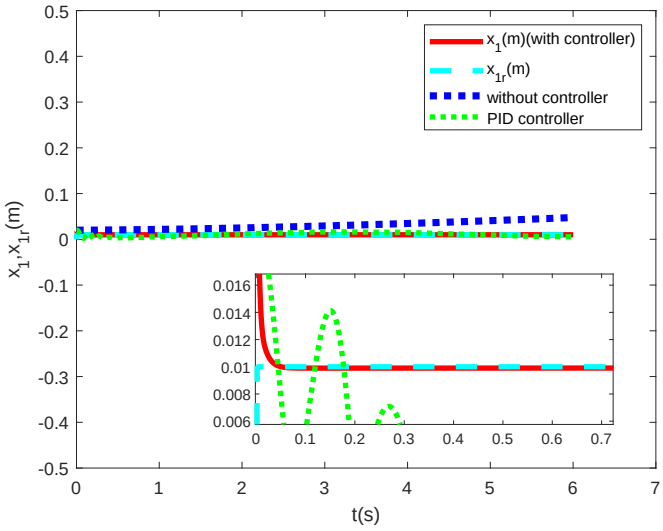

Figure 2. Tracing curve of vertical displacement of sprung mass.

Figure 4 is the state curve of car body speed. Compared with the design controller, the PID controller has greater fluctuation of the speed curve. The corresponding system state error under the proposed control algorithm is shown in Figure 5. Combining Figure 4 and Figure 5, the car body completes the car body height adjustment with a smooth curve under the proposed control algorithm. The value of the system state error z_2 approaches 0 after a very short period of fluctuation.

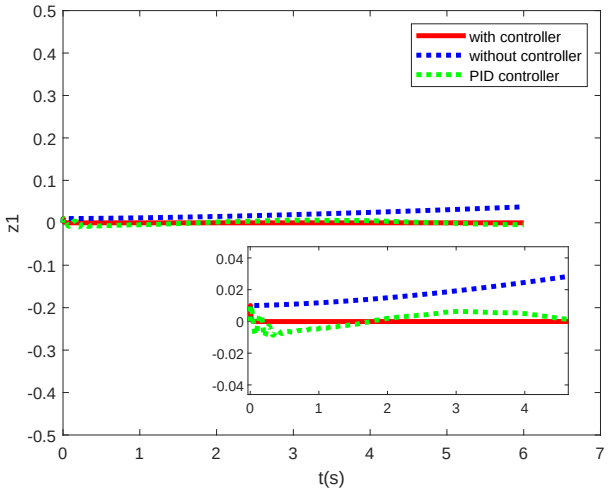

Figure 3. Tracing error curve of vertical displacement of sprung mass.

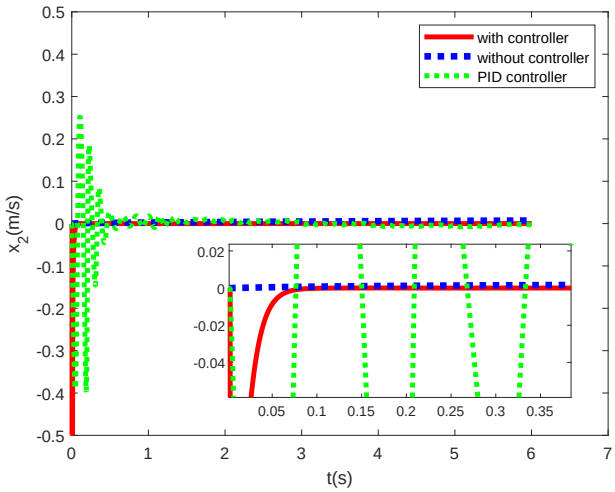

Figure 4. State curve of car body speed.

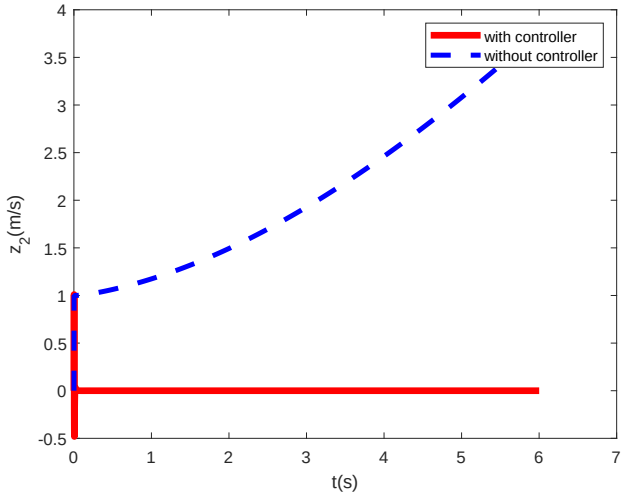

Figure 5. State curve of z_2.

Figure 6 is the state curve of car body acceleration. As shown in the picture, the value of x_6 approaches 0 and the fluctuation is small. Figure 7 is the state curve of the controller. However, in both figures, the PID controller takes longer to stabilize and has a larger fluctuation range. The simulation confirms that the controller can keep stable.

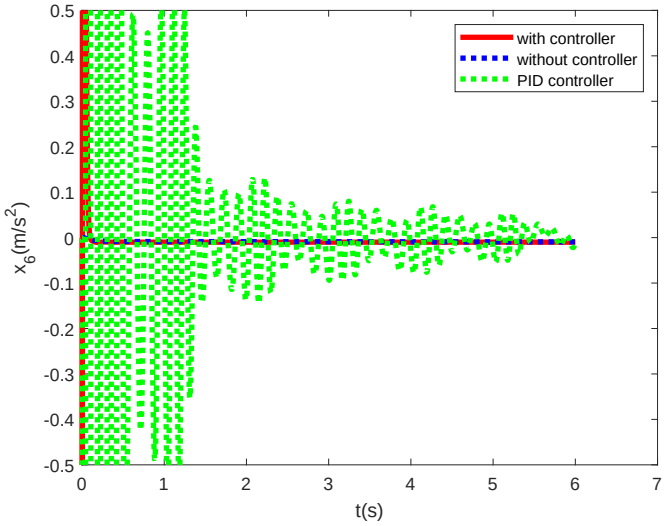

Figure 6. State curve of car body acceleration.

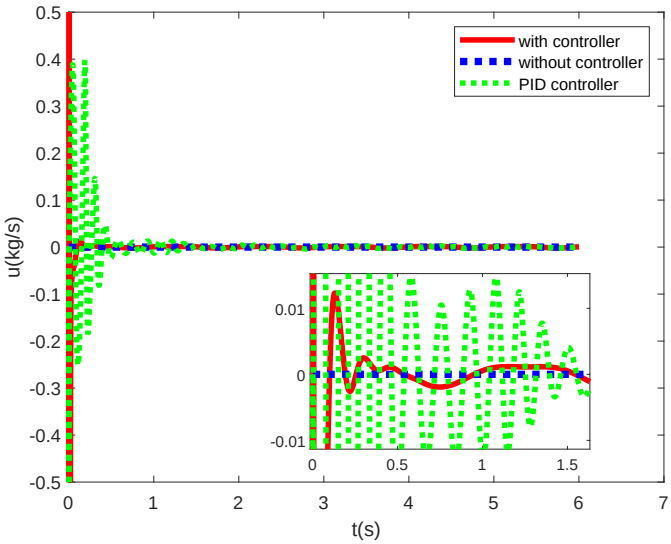

Figure 7. State curve of controller.

From Figures 2–7, the system remains stable under the control of the controller, which shows that the control algorithm is effective. Compared with the PID controller, the designed controller achieves better control effects.

3.2. Random Road Input

In the process of the random input of pavement simulation, the vertical input of the pavement is filtered white noise (Figure 8)

$$\dot{z}_r(t) = -2\pi n_1 v z_r(t) + 2\pi n_0 \sqrt{G_q(n_0) v w(t)} \tag{21}$$

The parameters are set as follows. n_1 is the lower cutoff frequency, v is speed of the car, n_0 is the spatial reference frequency, and $G_q(n_0)$ is the coefficient of road roughness. Class A uneven pavement is used in the simulation, where $n_0 = 0.1\ \mathrm{m}^{-1}, G_q(n_0) = 16 \times 10^{-6}\ \mathrm{m}^3, n_1 = 0.01\ \mathrm{m}^{-1}$, and $v = 10\ \mathrm{m}/s$.

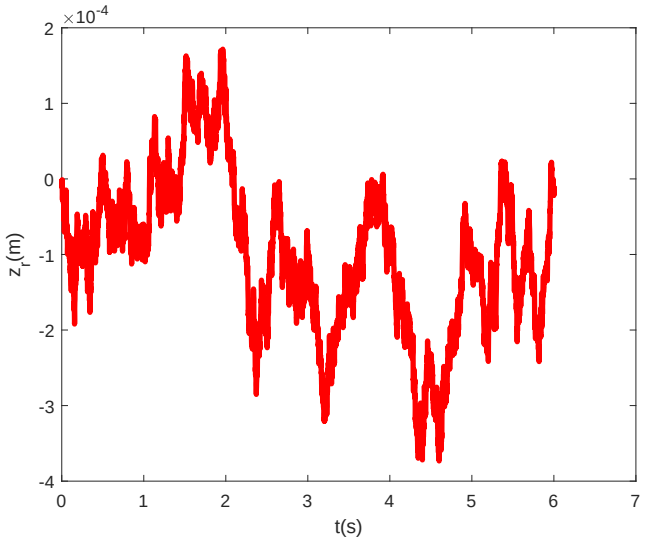

Figure 8. Vertical input for Class A uneven road surface.

The vehicle height was adjusted under a vertical input of $z_r = 0.01 \sin 2\pi t$ and an initial height of air sprung $z_{a0} = 0.03$ m; the uncertain outer boundary perturbation input $F_1(t) = F_2(t) = 0.01$, all states are initialized to 0, and the sampling time is 0.001 s.

The simulation results are shown in Figures 9–13. Figure 9 presents the difference between the state curves for the vehicle body height with and without the controller. Under the control of the controller, the state curves for the vehicle body height still have a certain level of fluctuation, but it is too small to be seen. Figure 10 shows the state curves for the vehicle body height tracking error. Combining the two figures, it can be seen that the controller can effectively reduce the variation range of the process of the car body height adjustment, which means that the controller reduces the car body vibration created by the road input.

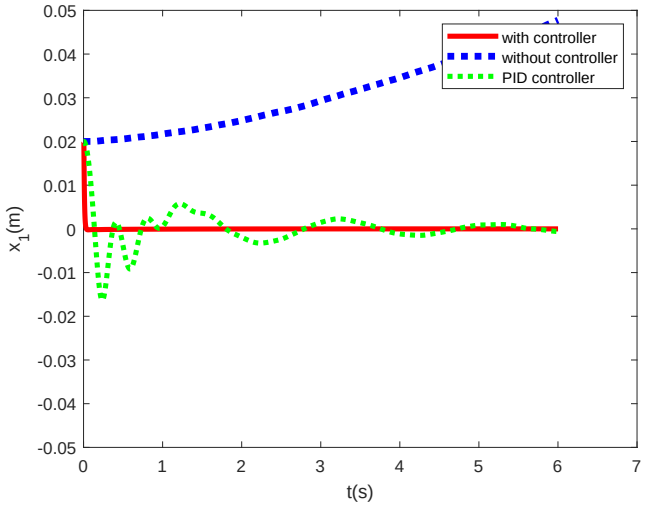

Figure 9. State curves for the vehicle body height.

Figure 11 shows the state curves for vehicle body velocity. During the process of car body height adjustment, the value of the vehicle body velocity increases and changes greatly. In contrast, the state curves for the vehicle body velocity keep stable under the control of the controller. However, like x_1, x_2 has small fluctuations but they are too small to be seen.

Figure 12 shows the state curves for the vehicle body acceleration. With the designed controller, the vertical acceleration of the body is reduced and thus, the comfort is improved. Under the condition of no controller, the fluctuation of the vehicle body acceleration state curve is large. The PID controller cannot reduce the fluctuation amplitude of the

body acceleration curve. Compared with the PID controller, the designed controller is more efficient.

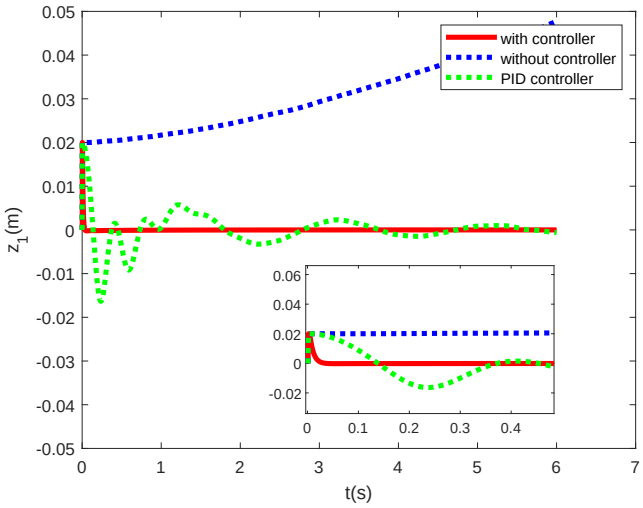

Figure 10. State curves for the vehicle body height tracking error.

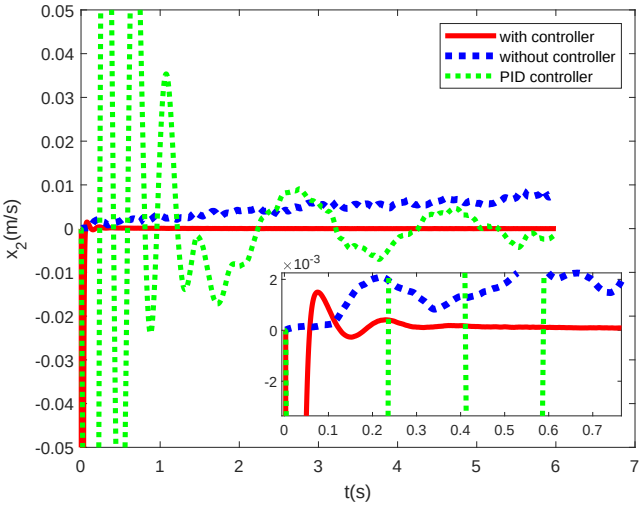

Figure 11. State curves for the vehicle body velocity.

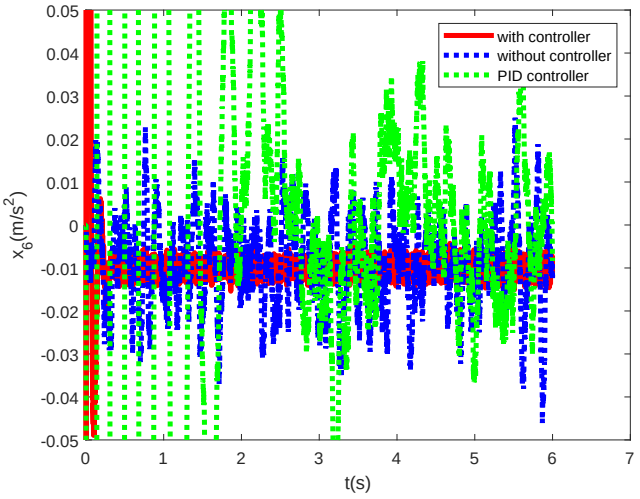

Figure 12. State curves for the vehicle body acceleration.

In the process of the vehicle body height adjustment, the state curves of the controller are shown in Figure 13. Compared with the PID controller, the designed controller has a shorter settling time and faster stabilization.

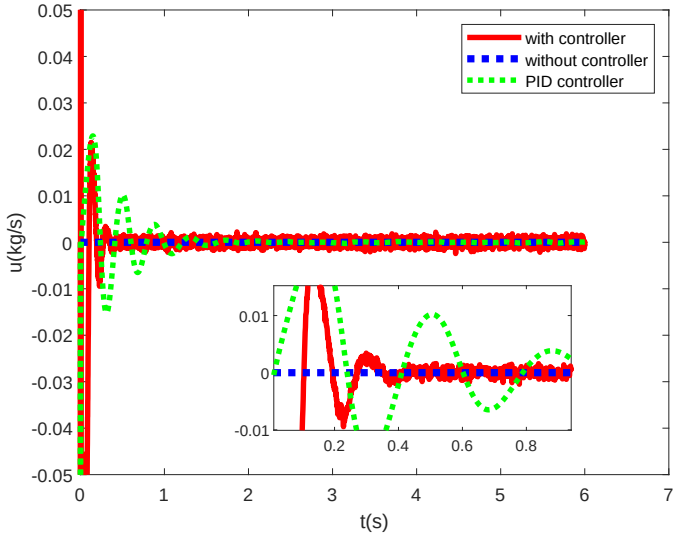

Figure 13. State curves of the controller.

4. Conclusions

In this paper, an adaptive control algorithm for the vehicle height adjustment of nonlinear air suspensions is proposed to improve the vehicle ride comfort. The designed algorithm can track the reference height curve, and the stability of the nonlinear air suspension systems with uncertainties is guaranteed by Lyapunov stability theory. Two different simulations are carried out to verify the effectiveness of the proposed controller. In the case of sinusoidal road input, the controller can track the reference value of body height well and make the corresponding error tend to 0. In the case of random road input, the controller reduces the fluctuation of the vertical parameters and improves the ride comfort. The following research will focus on the experimental verification of the proposed controller.

Author Contributions: Methodology, J.Z.; Writing—original draft, Y.Y.; Funding acquisition, C.H. All authors have read and agreed to the published version of the manuscript.

Funding: This research was funded by the Guangzhou Science and Technology Plan Project (202201010475, 202201020173) and the National Natural Science Foundation of China (52202492).

Data Availability Statement: The data used to support the findings of this study are included within the article.

Conflicts of Interest: The authors declare no conflict of interest.

References

1. Zhang, J.; Sun, W.; Du, H. Integrated Motion Control Scheme for Four-Wheel-Independent Vehicles Considering Critical Conditions. *IEEE Trans. Veh. Technol.* **2019**, *68*, 7488–7497. [CrossRef]
2. Jin, X.; Wang, J.; Sun, S.; Li, S.; Yang, J.; Yan, Z. Design of Constrained Robust Controller for Active Suspension of In-Wheel-Drive Electric Vehicles. *Mathematics* **2021**, *9*, 249. [CrossRef]
3. Jin, X.; Wang, J.; Yang, J. Development of Robust Guaranteed Cost Mixed Control System for Active Suspension of In-Wheel-Drive Electric Vehicles. *Math. Probl. Eng.* **2022**, *2022*, 4628539. [CrossRef]
4. Fu, Z.J.; Dong, X.Y. H infinity optimal control of vehicle active suspension systems in two time scales. *Automatika* **2021**, *62*, 284–292. [CrossRef]
5. Zhang, J.; Sun, W.; Feng, Z. Vehicle yaw stability control via H∞ gain scheduling. *Mech. Syst. Signal Process.* **2018**, *106*, 62–75. .: 10.1016/j.ymssp.2017.12.033. [CrossRef]
6. Veselov, G.; Sinicyn, A. Synthesis of sliding control system for automotive suspension under kinematic constraints. *J. Vibroeng.* **2021**, *23*, 1446–1455. [CrossRef]

7. Zhang, W.; Fan, X. Observer-based event-triggered control and application in active suspension vehicle systems. *Syst. Sci. Control Eng.* **2022**, *10*, 282–288. [CrossRef]
8. Unguritu, M.G.; Nichitelea, T.C.; Selisteanu, D. Design and Performance Assessment of Adaptive Harmonic Control for a Half-Car Active Suspension System. *Complexity* **2022**, *2022*, 3190520. [CrossRef]
9. Wu, K.; Ren, C. Control and Stability Analysis of Double Time-Delay Active Suspension Based on Particle Swarm Optimization. *Shock Vib.* **2020**, *2020*, 8873701. [CrossRef]
10. Zhang, J.; Sun, W.; Jing, H. Nonlinear Robust Control of Antilock Braking Systems Assisted by Active Suspensions for Automobile. *IEEE Trans. Control Syst. Technol.* **2019**, *27*, 1352–1359. [CrossRef]
11. Pan, F.; Luo, J.; Wu, W. Active Disturbance Rejection Control of Voice Coil Motor Active Suspension Based on Displacement Feedback. *Actuators* **2022**, *11*, 351. [CrossRef]
12. Fu, B.; Giossi, R.L.; Persson, R.; Stichel, S.; Bruni, S.; Goodall, R. Active suspension in railway vehicles: A literature survey. *Railw. Eng. Sci.* **2020**, *28*, 3–35. [CrossRef]
13. Jiang, H.; Xu, G.; Zeng, W.; Gao, F.; Chong, K. Lateral Stability of a Mobile Robot Utilizing an Active Adjustable Suspension. *Appl. Sci.* **2019**, *9*, 4410. [CrossRef]
14. Zhang, J.; Sun, W.; Liu, Z.; Zeng, M. Comfort braking control for brake-by-wire vehicles. *Mech. Syst. Signal Process.* **2019**, *133*, 106255. [CrossRef]
15. Zhang, J.; Wang, M. Integrated Adaptive Steering Stability Control for Ground Vehicle with Actuator Saturations. *Appl. Sci.* **2022**, *12*, 8502. [CrossRef]
16. Gao, S.; Zhang, B.; Sun, J. Research on the Design Method of a Bionic Suspension Workpiece Based on the Wing Structure of an Albatross. *Appl. Bionics Biomech.* **2019**, *2019*, 2539410. [CrossRef]
17. Rui, B. Nonlinear adaptive sliding-mode control of the electronically controlled air suspension system. *Int. J. Adv. Robot. Syst.* **2019**, *16*, 1729881419881527. [CrossRef]
18. Ha, D.V.; Tan, V.V.; Niem, V.T.; Sename, O. Evaluation of Dynamic Load Reduction for a Tractor Semi-Trailer Using the Air Suspension System at all Axles of the Semi-Trailer. *Actuators* **2022**, *11*, 12. [CrossRef]
19. Chen, B.; Dong, G.; Shi, Y.; Tan, X.Y. Research on Damping Mode of Passenger Vehicle Air Suspension System. In Proceedings of the 3rd International Workshop on Renewable Energy and Development (IWRED), Guangzhou, China, 8–10 March 2019; Volume 267. [CrossRef]
20. Sun, L.; Wang, Y.; Li, Z.; Geng, G.; Liao, Y.G. H-infinity Robust Control of Interconnected Air Suspension Based on Mode Switching. *IEEE Access* **2022**, *10*, 62377–62390. [CrossRef]
21. Li, Z.; Zhou, Y.; Zhang, X.; Jiang, H.; ; Xue, H. Interconnected State Control Method and Simulations of Four-corner Interconnected Air Suspension. In Proceedings of the 6th International Conference on Mechanical, Materials and Manufacturing (ICMMM), Boston, MA, USA, 12–14 October 2019; Volume 689. [CrossRef]
22. Zhao, Y.; Sun, X.; Wang, G.; Fan, Y. Adaptive Backstepping Sliding Mode Tracking Control for Underactuated Unmanned Surface Vehicle With Disturbances and Input Saturation. *IEEE Access* **2021**, *9*, 1304–1312. [CrossRef]
23. Qian, F.; Cai, J.; Wang, B.; Yu, R. Adaptive Backstepping Control for a Class of Nonlinear Systems with Unknown Time Delay. *IEEE Access* **2020**, *8*, 229–236. [CrossRef]
24. Jeon, B.J.; Seo, M.G.; Shin, H.S.; Tsourdos, A. Closed-loop Analysis with Incremental Backstepping Controller considering Measurement Bias. *IFAC Pap.* **2019**, *52*, 405–410. [CrossRef]
25. Brummelhuis, K.; Saikumar, N.; Van Wingerden, J.W.; HosseinNia, S.H. Adaptive Feedforward Control For Reset Feedback Control Systems—Application in Precision Motion Control. In Proceedings of the 2021 European Control Conference (ECC), Delft, The Netherlands, 29 Jun–2 July 2021; pp. 2450–2457.
26. Alwan, N.A.S.; Hussain, Z.M. Deep Learning for Robust Adaptive Inverse Control of Nonlinear Dynamic Systems: Improved Settling Time with an Autoencoder. *Sensors* **2022**, *22*, 5935. [CrossRef]
27. Quang, L.H.; Putov, V.V.; Sheludko, V.N. Adaptive robust control of a multi-degree-of-freedom mechanical plant with resilient properties. In Proceedings of the 14th International Symposium on Intelligent Systems, ELECTR NETWORK, Montreal, QC, Canada, 14–16 December 2020; Zelinka, I., Pereira, F., Das, S., Ilin, A., Diveev, A., Nikulchev, E., Eds., 2021; Volume 186, pp. 611–619. [CrossRef]
28. Sun, W.; Zhang, J. Heavy Vehicle Air Suspension Control Considering Ride Comfort and Height Regulation. *Control Theory Appl.* **2022**, *39*, 1002–1010.